European Journal of Control (2004)10:411–420

European Journal of Control

Port-Based Asymptotic Curve Tracking for Mechanical Systems

Vincent Duindam and Stefano Stramigioli*

Control Laboratory, Faculty of EEMCS, University of Twente, P.O. Box 217, 7500 AE Enschede, The Netherlands

We examine the control problem of curve-tracking for a fully actuated mechanical system. Using a coordinate transformation on the momentum variables, we split the kinetic energy of the system in a desired and an undesired part, and then design an (intrinsically passive) controller as an interconnection of port-Hamiltonian subsystems, in such a way that asymptotic convergence to the desired curve is obtained. We illustrate the performance in a simulation.

Keywords: Hamiltonian Control Systems; Mechanical Systems; Nonlinear Control

1. Introduction

Traditional robot motion control tries to make a robot follow a reference point as closely as possible, as this reference point moves in space over time. Although this approach is a very sensible choice for many applications, there are also applications (e.g. contour following) for which the time aspect of the task is not so important, and the task is much more to stay on a certain curve at all times; the exact position in time is not directly important, as long as it is somewhere on this desired curve.

For this task, traditional controllers like PID cannot be applied directly, since there is no clearly defined error signal between the actual and desired position. Instead, a very elegant approach (a form of stiffness/impedance control as presented in Refs [6,11,16]) is to build a virtual potential field around the desired curve, such that the potential energy is minimal everywhere on the desired curve, and increases as the deviation from the desired curve increases (Fig. 1). The gradient of the potential field then gives the control torque to be applied to the robot, such that the robot moves as if a spring is pulling it in the direction of the desired curve.

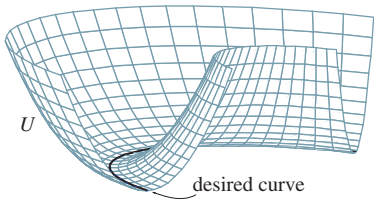

Fig. 1. The desired curve and a potential field U with gradient towards the desired curve.

Although this approach to curve tracking is very elegant and features many desirable properties like passivity, intuitive interpretation, and intuitive tuning, the performance is not so spectacular. The reason is that centrifugal and Coriolis forces drive the robot away from the minimum, and the potential field only produces a correcting torque after the robot has already deviated from the desired curve.

In this paper, we extend this potential field controller and improve the performance, without destroying the features like passivity and intuitive interpretation. We add control terms that are power-continuous (i.e. they do not change the energy) but

*E-mail: s.stramigioli@ieee.org
Correspondence to: V. Duindam. E-mail: v.duindam@ieee.org

Received 15 January 2004; Accepted 15 October 2004.
Recommended by A. Astolfi and A.J. Van der Schaft.

change the distribution of kinetic energy over the various (desired and undesired) directions to obtain asymptotic convergence.

The control law in this paper is based on the controller described in Ref. [3] and partially in Ref. [5], but the results have been completely reformulated in terms of an interconnection of port-Hamiltonian systems. The main advantage of this formulation is that the structure of the equations directly reveals energy storage and possible energy flows inside the system. Furthermore, the approach is suitable for modular controller design; we construct the total controller as a port-interconnection of subcontrollers for specific subtasks.

The control idea in this paper is also related to the passive velocity field control (PVFC) strategy described in Refs [8,9], but the main differences are (1) PVFC uses temporal energy storage in the form of a virtual flywheel whereas our approach is power-continuous, and (2) PVFC uses a cleverly chosen vector field to obtain convergence to a single curve where we use the potential field and extra power-continuous terms to obtain this convergence.

This paper is organized as follows. Section 2 gives the necessary mathematical preliminaries for the rest of the paper. Section 3 presents a derivation of the port-based control law, the main result of this paper. Section 4 then shows the behavior of the controller in a simulation. Finally, Section 5 gives the main conclusions and a discussion on possible directions for future research.

2. Preliminaries

In this section, we discuss the mathematical background knowledge necessary for the rest of the paper.

2.1. Manifolds and Tensors

We denote a differentiable manifold by Q, its points by q, and its dimension by $n \in \mathbb{N}$. The tangent bundle TQ of Q is the union of the tangent spaces T_qQ at all points $q \in Q$. Similarly, the cotangent bundle T^*Q of Q is the union of all cotangent spaces T_q^*Q. The intrinsic dual product between an element $v \in T_qQ$ and an element $\alpha \in T_q^*Q$ is denoted by $\langle v|\alpha\rangle \in \mathbb{R}$.

A $\mathcal{C}^\infty$ tensor field $T^{(k)}_{(l)}$ is a $\mathcal{C}^\infty$ mapping which assigns to each point $q \in Q$ a tensor of order k contravariant and order l co-variant (a type (k,l) tensor) such that the mapping

$$T(q) : \underbrace{T_qQ \times \cdots \times T_qQ}_{l \text{ times}} \times \underbrace{T_q^*Q \times \cdots \times T_q^*Q}_{k \text{ times}} \to \mathbb{R}$$

is linear in all its arguments at all $q \in Q$. Tensor fields can locally be expressed using coordinates, for example, T^{xy}_{vw} expresses the value of T acting on the basis vectors $\partial_v, \partial_w \in TQ$ and $\mathrm{d}x, \mathrm{d}y \in T^*Q$. We use the Einstein summation convention, which means that repetition of an index (once upper, once lower) implies summation over that index. Furthermore, we denote the partial derivative of a tensor $T^{(k)}_{(l)}$ to q^i by $T^{(k)}_{(l),i}$.

A Riemannian metric tensor field (denoted by g or in coordinates by g_{ij}) assigns to each point a symmetric positive-definite two-covariant tensor. A manifold endowed with such a structure is called a Riemannian manifold. Using the metric, we denote the inner product of two tangent vectors as

$$\langle v, w\rangle_g = g_{ij}v^i w^j \in \mathbb{R} \quad v, w \in T_qQ.$$

The inverse of the metric defines a metric g^{-1} acting on elements of T_q^*Q as

$$\langle \alpha, \beta\rangle_{g^{-1}} = g^{ij}\alpha_i\beta_j \in \mathbb{R} \quad \alpha, \beta \in T_q^*Q.$$

2.2. Port-Hamiltonian Systems

A general explicit port-Hamiltonian system is a dynamical system that can be represented by a set of differential equations of the following form

$$\begin{aligned} \dot{x} &= (J(x) - R(x))\frac{\partial H(x)}{\partial x} + g(x)u, \\ y &= g^T(x)\frac{\partial H(x)}{\partial x} + (K(x) + S(x))u \end{aligned} \tag{1}$$

in which $x \in \mathcal{X}$ is the state, $H : \mathcal{X} \to \mathbb{R}$ is the (differentiable) energy function, $J(x)$ and $K(x)$ are skew-symmetric matrices (to model power-continuous elements), $R(x)$ and $S(x)$ are positive semi-definite matrices (to model dissipative elements), and $(u, y) \in \mathcal{U} \times \mathcal{U}^*$ is the port through which the system can interact with, for example, a controller. For systems of this form it is straightforward to show that $\dot{H} \leq \langle u|y\rangle$, that is, the system is passive with respect to the port (u, y) with storage function H. Several generalizations for this kind of systems exist, for example, implicit formulations, and we refer the interested reader to Refs [1,12].

In this paper, we consider the subclass of mechanical systems (with H the mechanical energy) and we start from a conservative simple mechanical system (a system for which the total energy is the sum of kinetic and potential energy). If we take the state to be an element of the cotangent bundle T^*Q, the dynamics

can be described by a port-Hamiltonian system of the form

$$\frac{\mathrm{d}}{\mathrm{d}t}\begin{bmatrix} q \\ p \end{bmatrix} = \begin{bmatrix} 0 & I \\ -I & 0 \end{bmatrix}\begin{bmatrix} \dfrac{\partial H}{\partial q} \\ \dfrac{\partial H}{\partial p} \end{bmatrix} + \begin{bmatrix} 0 \\ B \end{bmatrix} u,$$
$$y = \begin{bmatrix} 0 & B^T \end{bmatrix}\begin{bmatrix} \dfrac{\partial H}{\partial q} \\ \dfrac{\partial H}{\partial p} \end{bmatrix}, \tag{2}$$

where (q, p) are canonical coordinates on the cotangent bundle (generalized positions and momenta), and H equals

$$H(q,p) = \frac{1}{2}\langle p, p\rangle_{g^{-1}} + V(q). \tag{3}$$

The first term of H is the kinetic energy, the second term is the potential energy. Systems described in these coordinates (q, p) with J as shown are called symplectic systems.

2.3. Bond Graphs

Though not commonly known, bond graphs (introduced by Paynter [10]) can be very useful to analyze energy aspects of physical systems. We give a rough guide how to read and use a bond graph like the ones in Figs 2–7; interested readers are referred to Ref. [7] for a more accurate and complete introduction to bond graphs, and to [15] for the use of bond graphs in robotics.

The half-arrows called bonds represent energy connections between subparts, carrying dual variables (called effort and flow, for mechanical systems force and velocity) where the dual product between the two represents the power flowing in the direction of the arrow. The stroke on either side of the arrow indicates the signal direction of the effort (force); the signal direction of the flow (velocity) is then in the opposite direction. A single arrow represents a one-dimensional bond, a double arrow represents a multi-dimensional bond.

The $\mathbb{I}$s are inertial elements, which integrate the incoming effort (force) to get the internal state (momentum), and output the partial derivative of the energy function to the state (i.e. the velocity). Similarly, a $\mathbb{C}$-element represents an elastic element, integrating the incoming flow (velocity) to get the internal state (displacement), and output the partial derivative of the energy function to the state (i.e. elastic force).

Both an modulated transformer ($\mathbb{MTF}$)-element and an modulated gyrator ($\mathbb{MGY}$)-element establish a power-connection between two bonds, the coupling strength of which can be modulated by some external (matrix) signal X. For the $\mathbb{MTF}$ we have the relations $f_2 = Xf_1$ and $e_1 = X^{\mathrm{T}}e_2$, while for the $\mathbb{MGY}$ we have the relations $e_2 = Xf_1$ and $e_1 = X^{\mathrm{T}}f_2$ (which automatically makes both elements power-continuous; the total power flowing in on one bond is always instantaneously equal to the total power flowing out on the other bond). Furthermore, an $\mathbb{MGY}$ with only one bond represents an element for which $e_1 = Xf_1$ with X skew-symmetric, such that the total instantaneous power on that bond is always zero.

Finally, 0- and 1-junctions represent generalized Kirchhoff laws, that is, all connecting bonds on a 0-junction have equal effort, all connecting bonds on a 1-junction have equal flow, and the (signed) sum of the power on the bonds equals zero.

Throughout this paper, we use bond graphs to give a graphical illustration of the various equations; even though the equations contain all the results, it can be very helpful to look at the corresponding bond graph to get a direct intuitive physical idea of what is going on in terms of energy flows.

3. Controller Derivation

As stated in Section 1, the control goal is to make a certain simple mechanical system follow a prescribed curve in joint space, denoted by a submanifold $Q_d \subset Q$. In this section we develop a port-based controller that accomplishes this goal. The controller itself is again the port-interconnection of several parts, each of which has its own purpose that can be described in terms of energy flows.

Instead of immediately trying to tackle the problem of convergence to Q_d, we first relax the control goal as follows: we replace the single desired curve by a family of non-intersecting curves (one of which is Q_d), one through each point of Q, in the form of a smooth non-zero vector field on Q, which we denote by w. This automatically implies that we will take a local approach, since the topology of the configuration space as well as the shape of the specified desired curve can make it impossible to define such a vector field globally (e.g. on $\mathbb{S}^{2n}$ this is the famous 'hairy-ball theorem').

Since we have a positive-definite metric g on Q, we can also equivalently look at this family of curves as a (local) smooth submanifold of T^*Q by transforming the vector field of each point into a covector at that point and considering these covectors as elements of T^*Q.

The initial goal is now for the system to converge to this submanifold, that is, to build a controller that

forces all kinetic energy in the direction of the desired vector field. The main goal, convergence to the desired curve Q_d, is then obtained by introducing a suitable potential field, that is, by a form of classical energy shaping.

3.1. Change of Coordinates

The first step is to represent the system of the form (9) in different coordinates (q, α) instead of (q, p). So in other words, we use the same coordinates q for the configuration, but different coordinates α for the momenta. The first[1] coordinate represents the desired momentum direction, and the other coordinates represent the other directions. We choose a new set of basis vectors $h^a(q)$ for T_q^*Q such that[2]

1. Every element $p \in T_q^*Q$ can be written as a linear combination of $h^a(q)$ (i.e. it is a basis).
2. For all $a \in \{2, \ldots, n\}$ we have $\langle h^a | w(q) \rangle = 0$.
3. The set of $\{h^a\}(q)$ defines a (local) diffeomorphism between $\mathbb{R}^n$ and T_q^*Q. In coordinates, the mapping h_i^a relates $p \in T_q^*Q$ and $\alpha \in \mathbb{R}^n$ as
$$\begin{aligned} p_i &= h_i^a \alpha_a, \\ \alpha_a &= (h^{-1})_a^j p_j = \hat{h}_a^j p_j, \end{aligned} \tag{4}$$
where we defined $\hat{h} := h^{-1}$ for ease of notation.
4. The metric $\bar{g}$ on $\mathbb{R}^n$ induced by g and h, that is,
$$\bar{g}^{ab}(q) = h_i^a(q) g^{ij}(q) h_j^b(q) \tag{5}$$
is diagonal and independent of q.

Note that properties 1, 2, and 4 together imply that
$$g_{ij}(q) w^j(q) = \gamma(q) h_i^1(q) \tag{6}$$
for some $\gamma(q) \neq 0$, and hence also that $h^1(q)$ is a (scalar) multiple of $g(q)w(q)$.

This choice of coordinates means that we will (locally) write T^*Q as the product $Q \times \mathbb{R}^n$ with coordinates (q, α), and the energy $\bar{H}$ in these new coordinates can be written as
$$\begin{aligned} \bar{H}(q,\alpha) := H(q, h^a \alpha_a) &= \frac{1}{2} \langle h^a \alpha_a, h^b \alpha_b \rangle_{g^{-1}} + V(q) \\ &= \frac{1}{2} \bar{g}^{ab} \alpha_a \alpha_b + V(q) = \frac{1}{2} \langle \alpha, \alpha \rangle_{\bar{g}^{-1}} + V(q), \end{aligned}$$
which is just the sum of the potential energy and the kinetic energies of the components α in the directions defined by h. Furthermore, the first coordinate α_1 represents the momentum in the desired direction (and thus the corresponding energy $\frac{1}{2}\bar{g}^{11}(\alpha_1)^2$ is the energy in the desired direction) while the other coordinates α represent the momentum (and corresponding energy) in the undesired directions. This splitting relies on the induced metric $\bar{g}$ being diagonal, and hence the basis vectors h^a being orthogonal in the metric g^{-1}.

Given a certain choice of h satisfying the criteria (there are many choices, since there are many choices of orthogonal basis vectors with constant norm), we can rewrite the dynamic equations in the new coordinates as presented in the following theorem. The results and derivation are similar to the ones in Ref. [4], but now with an invertible mapping h. They are also highly related to Ref. [13], as discussed in Ref. [2].

Theorem 1. The mechanical system (the plant) defined by (2) with coordinate transformation defined by h as before can be written as
$$\begin{aligned} \frac{\mathrm{d}}{\mathrm{d}t} \begin{bmatrix} q^i \\ \alpha_a \end{bmatrix} &= \bar{J} \begin{bmatrix} \dfrac{\partial \bar{H}}{\partial q^j} \\ \dfrac{\partial \bar{H}}{\partial \alpha_b} \end{bmatrix} + \begin{bmatrix} 0 \\ \hat{h}_a^j B_j^k \end{bmatrix} u_k, \\ y^i &= \begin{bmatrix} 0 & B_j^i \hat{h}_b^j \end{bmatrix} \begin{bmatrix} \dfrac{\partial \bar{H}}{\partial q^j} \\ \dfrac{\partial \bar{H}}{\partial \alpha_b} \end{bmatrix}, \end{aligned} \tag{7}$$
where $\bar{H}(q,\alpha) := \frac{1}{2}\langle \alpha, \alpha \rangle_{\bar{g}^{-1}} + V(q)$ and
$$\bar{J} := \begin{bmatrix} 0 & \hat{h}_b^i \\ -\hat{h}_a^j & \hat{h}_a^j \left(h_{k,j}^c - h_{j,k}^c \right) \alpha_c \hat{h}_b^k \end{bmatrix}.$$

Proof. We want to transform the dynamic equations in terms of (q, p) coordinates to (q, α) coordinates. First note that from (4) we have
$$\begin{aligned} \frac{\partial \alpha_a}{\partial q^i} &= -\hat{h}_a^j h_{j,i}^c \alpha_c, \\ \frac{\partial \alpha_a}{\partial p_i} &= \hat{h}_a^i \end{aligned}$$
and hence
$$\dot{\alpha}_a = -\hat{h}_a^j h_{j,i}^c \alpha_c \dot{q}^i + \hat{h}_a^i \dot{p}_i.$$
On T^*Q, we should have $\bar{H}(q,\alpha) = H(q,p)$ and hence also
$$\begin{aligned} \frac{\partial H}{\partial q^i} &= \frac{\partial \bar{H}}{\partial q^i} + \frac{\partial \bar{H}}{\partial \alpha_b} \frac{\partial \alpha_b}{\partial q^i}, \\ \frac{\partial H}{\partial p_i} &= \frac{\partial \bar{H}}{\partial \alpha_b} \frac{\partial \alpha_b}{\partial p_i}. \end{aligned}$$

[1] We restrict the derivation to convergence to a (one-dimensional) curve. The results can be easily generalized to convergence to higher-dimensional submanifolds.
[2] See also the remark at the end of this section.

Combining these results, we obtain

$$\dot{q}^i = \frac{\partial H}{\partial p_i} = \frac{\partial \bar{H}}{\partial \alpha_b}\frac{\partial \alpha_b}{\partial p_i} = \frac{\partial \bar{H}}{\partial \alpha_b}\hat{h}_b^i,$$

$$\dot{\alpha}_a = -\hat{h}_a^j h_{j,k}^c \alpha_c \left(\hat{h}_b^k \frac{\partial \bar{H}}{\partial \alpha_b}\right) + \hat{h}_a^j \left(-\frac{\partial \bar{H}}{\partial q^j} + \frac{\partial \bar{H}}{\partial \alpha_b}\hat{h}_b^k h_{k,j}^c \alpha_c + B_j^k u_k\right),$$

$$y^i = B_j^i \frac{\partial \bar{H}}{\partial \alpha_b}\frac{\partial \alpha_b}{\partial p_j} = B_j^i \frac{\partial \bar{H}}{\partial \alpha_b}\hat{h}_b^j.$$

These equations can be expressed in matrix form as in the theorem. □

Before we continue, let us structure the equations (7) in matrix form as follows:

$$\frac{\mathrm{d}}{\mathrm{d}t}\begin{bmatrix} q \\ \alpha_1 \\ \alpha_2 \end{bmatrix} = \begin{bmatrix} 0 & \hat{h}_1^T & \hat{h}_2^T \\ -\hat{h}_1 & 0 & X \\ -\hat{h}_2 & -X^T & Y \end{bmatrix} \begin{bmatrix} \frac{\partial \bar{H}}{\partial q} \\ \frac{\partial \bar{H}}{\partial \alpha_1} \\ \frac{\partial \bar{H}}{\partial \alpha_2} \end{bmatrix} + \begin{bmatrix} 0 \\ \hat{h}_1 B \\ \hat{h}_2 B \end{bmatrix} u,$$

$$y = \begin{bmatrix} 0 & B^T\hat{h}_1^T & B^T\hat{h}_2^T \end{bmatrix} \begin{bmatrix} \frac{\partial \bar{H}}{\partial q} \\ \frac{\partial \bar{H}}{\partial \alpha_1} \\ \frac{\partial \bar{H}}{\partial \alpha_2} \end{bmatrix},$$

where Y is skew-symmetric, subscripts 1 and 2 denote the first (desired) and other (undesired) components, respectively, and where the energy can be written as

$$\bar{H}(q, \alpha_1, \alpha_2) = \tfrac{1}{2}\alpha_1^T \bar{g}_1^{-1}\alpha_1 + \tfrac{1}{2}\alpha_2^T \bar{g}_2^{-1}\alpha_2 + V(q),$$

since $\bar{g}$ is diagonal. When written in this form, the equations can be represented by the bond graph of Fig. 2. The kinetic energy in the system is now represented by two $\mathbb{I}$-elements: one (corresponding to $\bar{g}_1$) representing the energy in the direction of the desired vector field w, and one (corresponding to $\bar{g}_2$) representing the energy in the other directions. There is still an energy coupling between the two storage elements through the modulated gyrator X and the $\mathbb{C}$ (the potential energy), and furthermore the energy supplied through the port (u, y) can still flow to both storage elements. The first purpose of the controller to be developed is to break the power connection between the two storage elements and ensure that all energy eventually flows to the $\bar{g}_1$ storage element (which corresponds exactly to converge to motion in the desired direction).

Remark. Readers familiar with the concepts of Riemannian geometry may wonder whether it is always possible to find a basis h that induces a constant diagonal metric g. Indeed, in Riemannian geometry it is shown how coordinate transformations can give such an induced metric *only if* the original metric is differentially flat, which is in general not the case. However, in this case we use a transformation h only on the momenta variables, that is, it is *not* induced by a transformation on the q variables as is the case in the aforementioned Riemannian context. In our case, we just want to find a transformation h (smoothly varying in q) that transforms a symmetric positive-definite matrix g (smoothly varying in q) to a constant diagonal matrix, which is indeed always possible.

3.2. Nominal Control

With the system in new coordinates, we now derive the first controller part, the nominal controller, with the goal to remove the energy-coupling between the two energy storages (desired and undesired). From this point, we will assume the potential energy (represented by the $\mathbb{C}$ in Fig. 2) to have been compensated for, so the only energy in the plant is the kinetic energy. We propose the following controller (shown as a bond graph in Fig. 3).

Theorem 2. For the mechanical system (2) or in transformed coordinates (7) with $V(q) = 0$, the following controller is power-continuous and keeps the

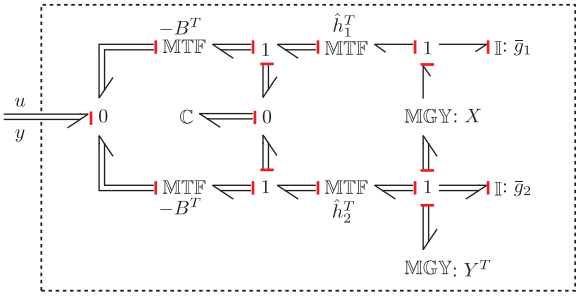

Fig. 2. Bond graph of the plant model in coordinates (q, α).

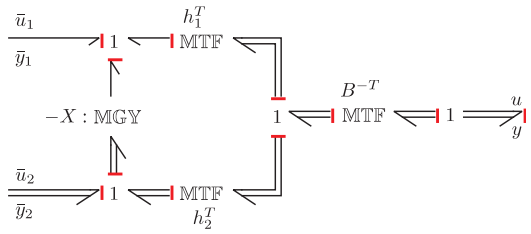

Fig. 3. Bond graph representation of the nominal controller.

kinetic energy of the system separated in two storage elements as defined by the mapping h.

$$\begin{bmatrix} u \\ \bar{y}_1 \\ \bar{y}_2 \end{bmatrix} = \begin{bmatrix} K & B^{-1}h_1 & B^{-1}h_2 \\ -h_1^{\mathrm{T}}B^{-\mathrm{T}} & 0 & 0 \\ -h_2 B^{-\mathrm{T}} & 0 & 0 \end{bmatrix} \begin{bmatrix} -y \\ \bar{u}_1 \\ \bar{u}_2 \end{bmatrix} \tag{8}$$

where K is a skew-symmetric matrix defined as

$$K = B^{-1}[\, h_1 \quad h_2 \,] \begin{bmatrix} 0 & X \\ -X^{\mathrm{T}} & 0 \end{bmatrix} \begin{bmatrix} h_1^{\mathrm{T}} \\ h_2^{\mathrm{T}} \end{bmatrix} B^{-\mathrm{T}}$$

and $(\bar{u}_1, \bar{y}_1)$ and $(\bar{u}_2, \bar{y}_2)$ are new control ports, one connected to each energy storage elements.

Proof. To prove power-continuity, we compute the power P_{in} going into the controller as well as the power P_{out} coming out:

$$P_{\text{in}} = \bar{u}_1^{\mathrm{T}}\bar{y}_1 + \bar{u}_2^{\mathrm{T}}\bar{y}_2 = \bar{u}_1^{\mathrm{T}}h_1^{\mathrm{T}}B^{-\mathrm{T}}y + \bar{u}_2^{\mathrm{T}}h_2^{\mathrm{T}}B^{-\mathrm{T}}y,$$
$$P_{\text{out}} = u^{\mathrm{T}}y = y^{\mathrm{T}}Ky + \bar{u}_1^{\mathrm{T}}h_1^{\mathrm{T}}B^{-\mathrm{T}}y + \bar{u}_2^{\mathrm{T}}h_2^{\mathrm{T}}B^{-\mathrm{T}}y,$$

which are clearly equal (by skew symmetry of K), proving power continuity.

To prove the energy separation property, we can compute the interconnected system as

$$\frac{\mathrm{d}}{\mathrm{d}t}\begin{bmatrix} q \\ \alpha_1 \\ \alpha_2 \end{bmatrix} = \begin{bmatrix} 0 & \hat{h}_1^T & \hat{h}_2^T \\ -\hat{h}_1 & 0 & 0 \\ -\hat{h}_2 & 0 & Y \end{bmatrix} \begin{bmatrix} \dfrac{\partial \bar{H}}{\partial q} \\ \dfrac{\partial \bar{H}}{\partial \alpha_1} \\ \dfrac{\partial \bar{H}}{\partial \alpha_2} \end{bmatrix} + \begin{bmatrix} 0 & 0 \\ 1 & 0 \\ 0 & I \end{bmatrix} \begin{bmatrix} \bar{u}_1 \\ \bar{u}_2 \end{bmatrix},$$

$$\begin{bmatrix} \bar{y}_1 \\ \bar{y}_2 \end{bmatrix} = \begin{bmatrix} 0 & 1 & 0 \\ 0 & 0 & I \end{bmatrix} \begin{bmatrix} \dfrac{\partial \bar{H}}{\partial q} \\ \dfrac{\partial \bar{H}}{\partial \alpha_1} \\ \dfrac{\partial \bar{H}}{\partial \alpha_2} \end{bmatrix}.$$

Since $V(q) = 0$, we have $\partial \bar{H}/\partial q = 0$, so the equations for $\dot{\alpha}_{1,2}$ and $\bar{y}_{1,2}$ reduce to

$$\dot{\alpha}_1 = \bar{u}_1,$$
$$\dot{\alpha}_2 = Y\bar{g}_2^{-1}\alpha_2 + \bar{u}_2,$$
$$\bar{y}_1 = \bar{g}_1^{-1}\alpha_1,$$
$$\bar{y}_2 = \bar{g}_2^{-1}\alpha_2,$$

which shows that indeed the two storage elements α_1 and α_2 are decoupled, and the two ports $(\bar{u}_1, \bar{y}_1)$ and $(\bar{u}_2, \bar{y}_2)$ act separately on the two storage elements.

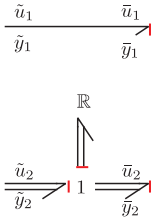

Fig. 4. Bond graph representation of the dissipative asymptotic controller.

3.3. Asymptotic Control

The interconnection of the plant with the nominal controller of the previous section results in two decoupled systems, one of which represents the desired motion, whereas the other represents the undesired motions. To obtain asymptotic convergence, we just need to reduce the energy in the undesired direction to zero.

We present two approaches to accomplish this goal: the first one uses straightforward dissipation, the second one uses a power-continuous interconnection.

3.3.1. Using Dissipation

The most straightforward way to reduce the energy in the α_2 subsystem is to dissipate it, that is, to apply the controller

$$\begin{bmatrix} \bar{u}_1 \\ \bar{u}_2 \\ \tilde{y}_1 \\ \tilde{y}_2 \end{bmatrix} = \begin{bmatrix} 0 & 0 & 1 & 0 \\ 0 & R & 0 & I \\ -1 & 0 & 0 & 0 \\ 0 & -I & 0 & 0 \end{bmatrix} \begin{bmatrix} -\bar{y}_1 \\ -\bar{y}_2 \\ \tilde{u}_1 \\ \tilde{u}_2 \end{bmatrix}$$

with R a positive-definite matrix. The controller is represented as a bond graph in Fig. 4. The power balance for this controller is

$$P_{\text{in}} = \tilde{u}_1^T\tilde{y}_1 + \tilde{u}_2^T\tilde{y}_2 = \tilde{u}_1^T\bar{y}_1 + \tilde{u}_2^T\bar{y}_2,$$
$$P_{\text{out}} = \bar{u}_1^T\bar{y}_1 + \bar{u}_2^T\bar{y}_2 = \tilde{u}_1^T\bar{y}_1 + \tilde{u}_2^T\bar{y}_2 - \bar{y}_2^T R\bar{y}_2,$$

which shows that $P_{\text{out}} \leq P_{\text{in}}$, so this controller is passive. Furthermore, if $\tilde{u}_2 = 0$ (i.e. no forces/torques are applied to the second port), then since $R > 0$, the kinetic energy in the second storage element (the undesired energy) decreases monotonically to zero, thus providing asymptotic convergence to the desired vector field.

3.3.2. Using Power-Continuous Control

Instead of dissipating the undesired energy as was done in the previous section, we can reuse the

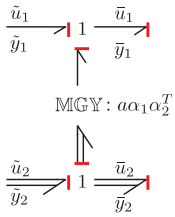

Fig. 5. Bond graph representation of the power continuous asymptotic controller.

undesired energy by pumping it to the desired direction. An example of such a controller is the following (with corresponding bond graph in Fig. 5).

$$\begin{bmatrix} \bar{u}_1 \\ \bar{u}_2 \\ \tilde{y}_1 \\ \tilde{y}_2 \end{bmatrix} = \begin{bmatrix} 0 & -a\alpha_1\alpha_2^T & 1 & 0 \\ a\alpha_2\alpha_1^T & 0 & 0 & I \\ -1 & 0 & 0 & 0 \\ 0 & -I & 0 & 0 \end{bmatrix} \begin{bmatrix} -\bar{y}_1 \\ -\bar{y}_2 \\ \tilde{u}_1 \\ \tilde{u}_2 \end{bmatrix} \tag{9}$$

with $a > 0$ a parameter. The power balance for this controller can be shown to give $P_{\text{in}} = P_{\text{out}}$, proving that this controller is power-continuous. More interestingly, we can compute the change of the kinetic energy in the two storage elements when this controller is connected (and both inputs $\tilde{u}_{1,2}$ are set to zero).

$$\frac{\mathrm{d}}{\mathrm{d}t}\left(\frac{1}{2}\langle\alpha_1,\alpha_1\rangle_{\bar{g}_1^{-1}}\right) = a\langle\alpha_1,\alpha_1\rangle_{\bar{g}_1^{-1}}\langle\alpha_2,\alpha_2\rangle_{\bar{g}_2^{-1}},$$
$$\frac{\mathrm{d}}{\mathrm{d}t}\left(\frac{1}{2}\langle\alpha_2,\alpha_2\rangle_{\bar{g}_2^{-1}}\right) = -a\langle\alpha_2,\alpha_2\rangle_{\bar{g}_2^{-1}}\langle\alpha_1,\alpha_1\rangle_{\bar{g}_2^{-1}},$$

which shows that whenever both α_1 and α_2 are nonzero, the undesired energy will decrease and the desired energy will increase. So, if the initial desired energy is nonzero (i.e. the system is moving at least a little bit in the desired direction), then the system will again converge to the desired vector field.

Remark. This particular choice of controller gives slow convergence because it is quadratic in α_2, so as α_2 approaches zero, the control force approaches zero even faster. This can be improved, for example, by replacing the parameter a by the expression

$$a \to \frac{a}{\sqrt{\langle\alpha_2,\alpha_2\rangle_{\bar{g}_2^{-1}} + \epsilon}}$$

for some small $\epsilon > 0$. We use this controller for the simulations of Section 4.

3.4. Potential Energy

The interconnection of the two power-continuous controllers of the previous section establishes asymptotic convergence to motion along the desired vector field w. So depending on the initial conditions, the system converges to motion along one of the integral curves of the vector field.

In this section, we add an artificial potential field $\bar{V}(\bar{q})$ (with $\bar{q} \in Q$) to the controller to obtain convergence to one specific integral curve, that is, Q_d. The function $\bar{V}$ has to satisfy the following properties

1. $\bar{V}$ is radially unbounded.
2. $\langle d\bar{V}|w\rangle = 0$ for all $q \in Q$ (with w the desired vector defined in Section 3).
3. $\bar{V}(q) \geq 0$ with equality if and only if $q \in Q_d$.

Given such a $\bar{V}$, we are ready to derive the final controller.

Theorem 3. Given the mechanical system (2 or in transformed coordinates (7) with $V(q) = 0$, and define a new controller as the interconnection of the nominal controller (8) with the asymptotic controller (9) and extend the nominal controller to become

$$\frac{\mathrm{d}}{\mathrm{d}t}\bar{q} = \begin{bmatrix} -B^{-T} & 0 & 0 \end{bmatrix} \begin{bmatrix} -y \\ \bar{u}_1 \\ \bar{u}_2 \end{bmatrix}$$
$$\begin{bmatrix} u \\ \bar{y}_1 \\ \bar{y}_2 \end{bmatrix} = \begin{bmatrix} K & B^{-1}h_1 & B^{-1}h_2 \\ -h_1^T B^{-T} & 0 & 0 \\ -h_2 B^{-T} & 0 & 0 \end{bmatrix} \begin{bmatrix} -y \\ \bar{u}_1 \\ \bar{u}_2 \end{bmatrix} + \begin{bmatrix} -B^{-1} \\ 0 \\ 0 \end{bmatrix} \frac{\partial \bar{V}}{\partial \bar{q}}$$

with $\bar{V}$ satisfying the properties discussed above. Let the initial conditions be such that $\bar{q}(0) = q(0)$, $\alpha_1(0) \neq 0$, and that

$$\bar{H}(q(0),\alpha(0)) + \bar{V}(\bar{q}(0)) < \bar{V}(q_x)$$

for all q_x in $\{q \in Q | dV(q) = 0, q \notin Q_d\}$. Then the closed loop system converges asymptotically to Q_d, while the total energy $\bar{H}(q,\alpha) + \bar{V}(\bar{q})$ is constant.

Proof. Figure 6 shows a bond graph of the total controller, and it can be seen that the extended version of the nominal controller just means the addition of a $\mathbb{C}$ element (with state $\bar{q}$ and energy function $\bar{V}(\bar{q})$). From (2) we can see that $(\mathrm{d}/\mathrm{d})t\bar{q} = \dot{q}$, so if $\bar{q}(0) = q(0)$, then $\bar{q} = q$ at all times.[3] In the following, we assume $\bar{q} = q$ and write $\bar{V}$ as a function of q accordingly.

[3]This means that $q - \bar{q}$ will be a Casimir function of the closed-loop system.

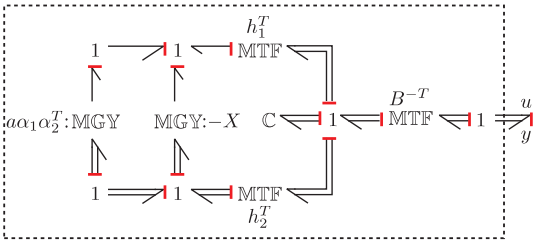

Fig. 6. Bond graph representation of the complete controller.

The closed-loop equations of the controller interconnected to the plant can be computed as

$$\frac{\mathrm{d}}{\mathrm{d}t}\begin{bmatrix} q \\ \alpha_1 \\ \alpha_2 \end{bmatrix} = \begin{bmatrix} 0 & \hat{h}_1^{\mathrm{T}} & \hat{h}_2^{\mathrm{T}} \\ -\hat{h}_1 & 0 & a\alpha_1\alpha_2^{\mathrm{T}} \\ -\hat{h}_2 & -a\alpha_2\alpha_1^{\mathrm{T}} & Y \end{bmatrix} \begin{bmatrix} \dfrac{\partial \bar{V}}{\partial q} \\ \dfrac{\partial \bar{H}}{\partial \alpha_1} \\ \dfrac{\partial \bar{H}}{\partial \alpha_2} \end{bmatrix},$$

which again can be represented as a bond graph, shown in Fig. 7. It can be seen that if $\bar{q} = q$, then both bonds connected to the MTF-element labeled $\hat{h}_1^{\mathrm{T}}$ have zero power flowing through them (and hence $\hat{h}_1 d\bar{V} = 0$).

The fact that the closed-loop system is Hamiltonian immediately proves energy conservation. To prove asymptotic convergence to the desired curve, we propose the following candidate Lyapunov function $\mathcal{L}$:

$$\mathcal{L}(q,\alpha) := \tfrac{1}{2}\langle \alpha_2, \alpha_2 \rangle_{\bar{g}_2^{-1}} + \bar{V}(q),$$

so the Lyapunov function precisely equals the undesired kinetic energy (associated with deviation from motion along the vector field) plus the virtual potential energy (associated with deviation from the desired curve), and it is positive definite. We compute its time derivative as

$$\begin{aligned} \frac{\mathrm{d}}{\mathrm{d}t}\mathcal{L}(q,\alpha) &= \frac{\partial^T \bar{V}}{\partial q}\dot{q} + \alpha_2^T \bar{g}_2^{-1}\dot{\alpha}_2 \\ &= \frac{\partial^T \bar{V}}{\partial q}\left(\hat{h}_1^T \bar{g}_1^{-1}\alpha_1 + \hat{h}_2^T \bar{g}_2^{-1}\alpha_2\right) \\ &\quad + \alpha_2^T \bar{g}_2^{-1}\left(Y\bar{g}_2^{-1}\alpha_2 - \hat{h}_2 \frac{\partial \bar{V}}{\partial q} - a\alpha_2\alpha_1^T \bar{g}_1^{-1}\alpha_1\right) \\ &= -a\langle \alpha_1, \alpha_1 \rangle_{\bar{g}_1^{-1}} \langle \alpha_2, \alpha_2 \rangle_{\bar{g}_2^{-1}}, \end{aligned}$$

where we used the second property of $\bar{V}$ and skew-symmetry of Y. Thus, $(\mathrm{d}/\mathrm{d}t)\mathcal{L}$ is negative everywhere except in the set

$$E := \{(q,\alpha_1,\alpha_2) | \alpha_1 = 0 \text{ and/or } \alpha_2 = 0\}.$$

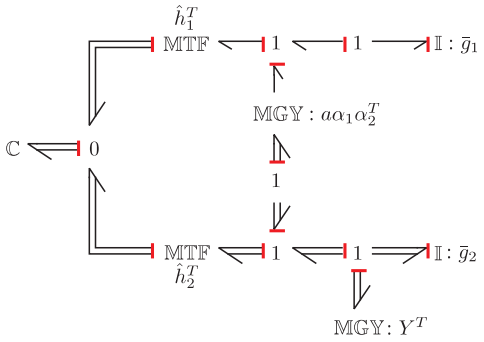

Fig. 7. Bond graph representation of the closed-loop system.

We now look for the largest invariant set in E. For $\alpha_1 = 0$ and/or $\alpha_2 = 0$ we can compute

$$\begin{aligned} \dot{\alpha}_1 &= \hat{h}_1 dV = 0, \\ \dot{\alpha}_2 &= \hat{h}_2 dV + Y^T \bar{g}_2^{-1}\alpha_2, \end{aligned}$$

which shows that the largest invariant set M in E is

$$M = \{(q,\alpha_1,\alpha_2) | \alpha_1 = 0 \text{ or } (\alpha_2 = 0 \text{ and } dV = 0)\}.$$

Now first consider the first part; $\alpha_1 = 0$. By energy conservation and the fact that $\mathcal{L}$ is decreasing, we have that the desired kinetic energy increases over time, implying that also $\langle \alpha_1, \alpha_1 \rangle$ can only increase over time. So once $\alpha_1 \neq 0$, it will never become zero again. In other words, if initially the system has (even a very slight) motion in the desired direction, then the condition $\alpha_1 = 0$ will never be satisfied and the system will never get stuck in that condition.

So given this (mild) restriction on initial conditions, the only invariant set in E left is the one where $d\bar{V} = 0$ and $\alpha_2 = 0$. Given furthermore the condition that the total (initial) energy is less than $\bar{V}(q_x)$ for all q_x in the given set, it follows that Q_d is the only reachable set for which $d\bar{V} = 0$. So indeed, the only invariant set in E is the one for which $\alpha_2 = 0$ and $q \in Q_d$. Hence, by the Local Invariant Set Theorem [14], the system converges asymptotically to the desired curve, which was to be proved.

Remark. The extra state $\bar{q}$ for the controller is only introduced for the theoretical proof of passivity. Computing this state by integrating the measured velocity in open loop is clearly very sensitive to drift, and hence in practice $\bar{q}$ will be estimated by directly measuring q, in which case the initial condition on $\bar{q}$ is void. Still, as in most proofs based on passivity, perfect transfer of port-variables between plant and controller is assumed, that is, perfect velocity sensors and perfect force actuators.

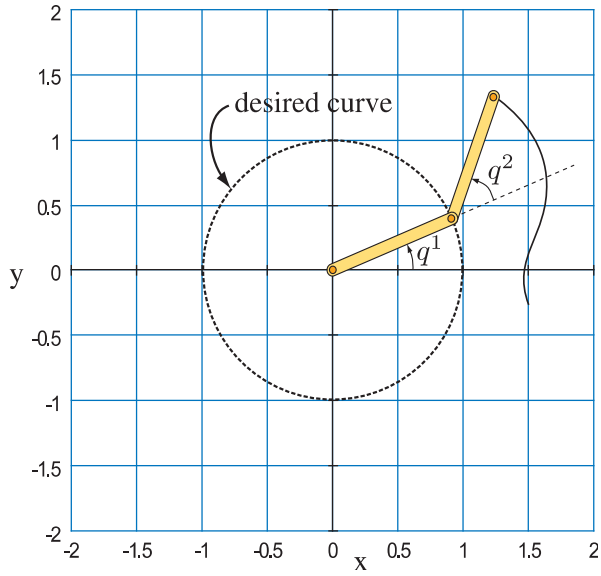

Fig. 8. Schematic view of the 2DoF manipulator that needs to be controlled to follow the unit circle.

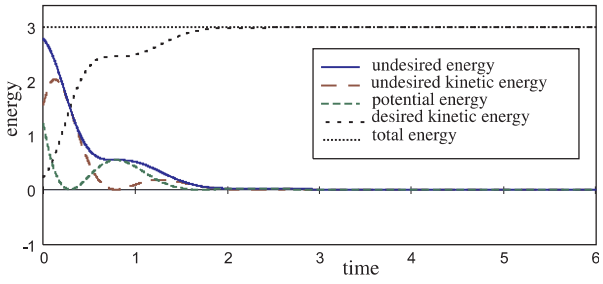

Fig. 9. Time-evolution of the various energies defined in Section 3; the undesired energy decreases to zero, while the total energy is constant.

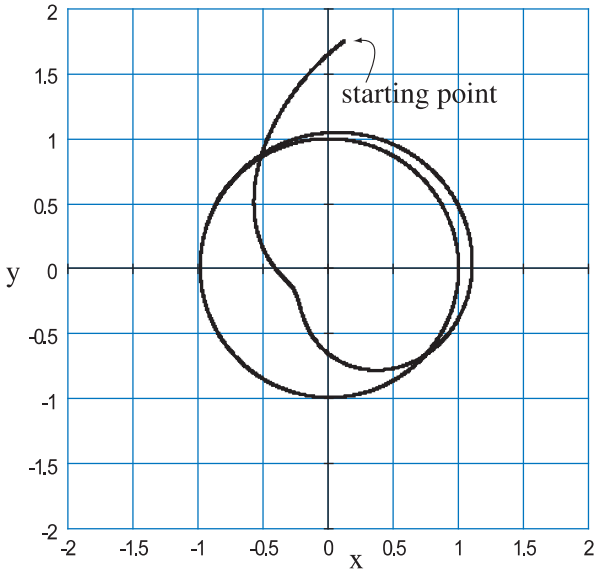

Fig. 10. Trajectory as traced by the end effector of the manipulator. It converges to motion along the unit circle, as desired.

4. Simulation Results

We demonstrate the behavior of the controller on a simple planar manipulator with two unit-length links, shown in Fig. 8. The goal is to make the end-effector trace the unit circle, which in joint space corresponds to the set of configurations with $q^2 = \frac{2}{3}\pi$ and q^1 arbitrary (we do not consider the second solution of $q^2 = -\frac{2}{3}\pi$ and q^1 arbitrary). As desired family of curves, we take all circles around the origin, which corresponds to the desired vector field $w(q) = [1 \quad 0]^{\mathrm{T}}$. We also choose the virtual potential field to be $\bar{V}(q) = \frac{1}{2}k(q^2 - \frac{2}{3}\pi)^2$. With these given, we apply the control algorithms from Section 3 (we choose the power-continuous asymptotic controller of Section 3.3.2) and simulate the behavior of the closed-loop system.

Figure 9 shows the resulting time-evolution of the various energies involved: the sum of virtual potential and undesired kinetic energy decreases monotonously, whereas the total (kinetic plus virtual potential) energy is constant at all times. Figure 10 shows the trace of the end-effector; starting from some initial configuration, it indeed converges to motion along the desired curve.

5. Conclusions and Future Work

5.1. Conclusions

In this paper, we used a port-based Hamiltonian approach to derive a controller that makes a mechanical system move along a reference trajectory. We first used a coordinates transformation to separate explicitly the desired and undesired motion. We then interconnected the system with two power-continuous controllers: one to decouple the desired energy flows from the undesired energy flows, and one to establish a unidirectional flow from the undesired energy storage element to the desired energy storage element, obtaining asymptotic convergence to motion along the integral curves of a vector field. Finally, we added an artificial potential field to obtain convergence to the one specified curve.

The controller was formulated as an interconnection of port-Hamiltonian subsystems; this representation directly exposed properties like passivity of the subsystems, and also showed where energy is stored and how energy can flow inside the system. Furthermore, the modularity of the port-based approach

allowed for example to design two sub-controllers for asymptotic convergence and just plug one of them into the total controller without altering the other parts.

5.2. Future Work

Future work is possible in several directions. First, the splitting in different desired and undesired directions can be directly generalized from desired curves to desired submanifolds, for example, to obtain convergence to a surface instead of a curve.

Second, the simplification was made here to have constant energy along the curve. An extension could be made to have a certain varying energy along the curve, the variations of which could then be stored temporarily in the controller, for example, in a $\mathbb{C}$-element or an $\mathbb{I}$-element (the latter would correspond to the virtual flywheel used in Ref. [8]).

Third, practical applications always suffer from friction which drains energy from the system. Therefore, a useful (non-passive) extension would be an additional control term that carefully adds or removes energy to or from the system, depending on the current and desired energy level. Passivity will be lost in this case, but energy balancing can still be taken into account carefully.

Fourth, we want to apply the results from this paper to the control of walking machines, in particular bipeds. This means that the approach should be extended to include impacts and state jumps, which occur when the feet of the robot come in contact with the ground.

Finally, several extensions can be made to account for systems which do not have full actuation or full state measurement. The results of this paper can also be combined with the results in Ref. [4] to include nonholonomic constraints.

Acknowledgement

This work has been done in the context of the European sponsored project GeoPlex with reference code IST-2001-34166. Further information is available at http://www.geoplex.cc.

References

1. Blankenstein G. *Implicit Hamiltonian systems: symmetry and interconnection*. PhD thesis, University of Twente, 2000
2. Duindam V, Blankenstein G, Stramigioli S. Port-based modeling and analysis of snakeboard locomotion. In: Proceeding of the International Symposium on Mathematical Theory of Networks and Systems, July 2004
3. Duindam V, Stramigioli S. Passive asymptotic curve tracking. In: Proceedings of the IFAC Workshop on Lagr. and Hamilt. Methods for Nonlinear Control, 2003, pp 229–234
4. Duindam V, Stramigioli S. Energy-based model-reduction and control of nonholonomic mechanical systems. In: Proceedings of the IEEE International Conference on Robotics and Automation, April 2004, pp 4584–4589
5. Duindam V, Stramigioli S, Scherpen JMA. Passive compensation of nonlinear robot dynamics. IEEE Trans. Robotics Automation, 2004; 20(3): 480–487
6. Hogan N. Impedance control: an approach to manipulation. J Dyn Syst Meas Contr 1985; 107(1): 1–24
7. Karnopp D, Margolis D, Rosenberg R. System dynamics, a unified approach. John Wiley and Sons, 1990
8. Li PY, Horowitz R. Passive velocity field control of mechanical manipulators. In: Proceedings of the IEEE International Conference on Robotics and Automation, 1995; pp 2764–2770
9. Li PY, Horowitz R. Passive velocity field control of mechanical manipulators. IEEE Trans. Robotics Automation 1999; 15(4): 751–763
10. Paynter HM. Analysis and design of engineering systems. MIT Press, 1961
11. Salisbury JK. Active stiffness control of a manipulator in Cartesian coordinates. In: Proceedings of the IEEE Conference on Decision and Control, 1980; pp 95–100
12. van der Schaft AJ. L_2-Gain and passivity techniques in nonlinear control. Communications and Control Engineering. Springer-Verlag, 2000
13. van der Schaft AJ, Maschke BM. On the Hamiltonian formulation of nonholonomic mechanical systems. Rep Math Phys 1994; 34: 225–233
14. Slotine JJE, Li W. Applied nonlinear control. Prentice-Hall, 1991
15. Stramigioli S. Modeling and IPC control of interactive mechanical systems – a coordinate-free approach. Springer-Verlag, 2001
16. Takegaki M, Arimoto S. A new feedback method for dynamic control of manipulators. J Dyn Syst Meas Contr 1981; 103(2): 119–125